# Automated tool for simulation of standardized tests of cohesive interfaces

## Petr Hanzlik[1,a], Tomas Kroupa[2,b]

[1]University of West Bohemia, Univerzitní 8, 301 00 Pilsen, Czech Republic

[2]University of West Bohemia, NTIS – New Technologies for the Information Society, Univerzitní 22, 301 00, Plzeň, Czech Republic

[a]petrhan@kme.zcu.cz, [b]kroupa@kme.zcu.cz

## Introduction

This work deals with determination of material parameters of cohesive interface using finite element models. Cohesive interface means conjunction of two deformable materials with relatively high stiffness compared to the interface. This conjunction or adhesive bonding determines overall strength of this system for certain loading types. In general, failure of such interface is caused by normal and shear stresses. Resulting failure is in fact a case of the crack growth and can be determined by parameters used in fracture mechanics. Strain energy release rate (SERR) $G$ was selected as a basic parameter for evaluation of cohesive interface failure for this reason. Numerical analyses are performed in FE software Abaqus 6.14. Automated tool for identification of material parameters of two of the mentioned basic modes was created using Python 2.7. programing language. Material parameters of two adhesives, Hunstman Araldite 2021 and Gurit Spabond 345, and an inner layer of laminated composite are identified through secondary material parameters: stiffness $k$, displacement $\delta^0$ (damage initiation) and $\delta^c$ (failure determination).

## Analytical models

General behaviour of loaded cohesive interface can be described using decomposition to three basic modes described on figure 1: Mode I – interface is loaded in the normal direction to a crack plane, Mode II – interface is loaded in the crack plane perpendicularly to a crack front, Mode III – load is in the direction of the crack front in the crack plane.
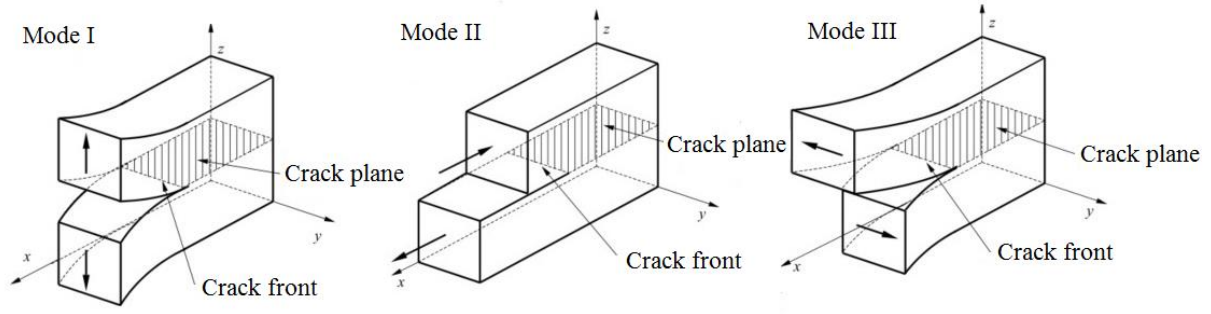
Figure 1: Basic modes of interface load [4]

As mentioned before, strain energy release rate (SERR) $G$ was selected as a basic parameter for evaluation of cohesive interface failure. This material parameter can be mathematically defined through strain energy $\pi$ as

$$G = -\frac{1}{b}\frac{d\pi}{da},\tag{1}$$

where $b$ is width of thin-walled specimen of standardized test and $a$ is length of interface crack. In case of cantilever beams equation 1 can be transformed into

$$G = \frac{F^2}{2b}\frac{dC}{da},\tag{2}$$

where $C$ is compliance of cantilever beam mathematically defined by displacement $\delta$ measured in place where load $F$ is applied as

$$C = \frac{\delta}{F}.\tag{3}$$

Crack growth is evaluated through Griffith criterion that can be summed up into four points [2]:

1. Crack grows when SERR is equal or exceeds its critical value $G^c$
2. At the moment of the crack growth are stresses in the area of growth constant.
3. Critical value of SERR is constant.
4. Crack grows in the direction of maximal component SERR.

Critical value of SERR is determined via analytical equations obtained by standardized tests. For load mode I the double cantilever beam test was used. For mode II end notched flexure test was used. For combination of mode I and II MMF test was used.
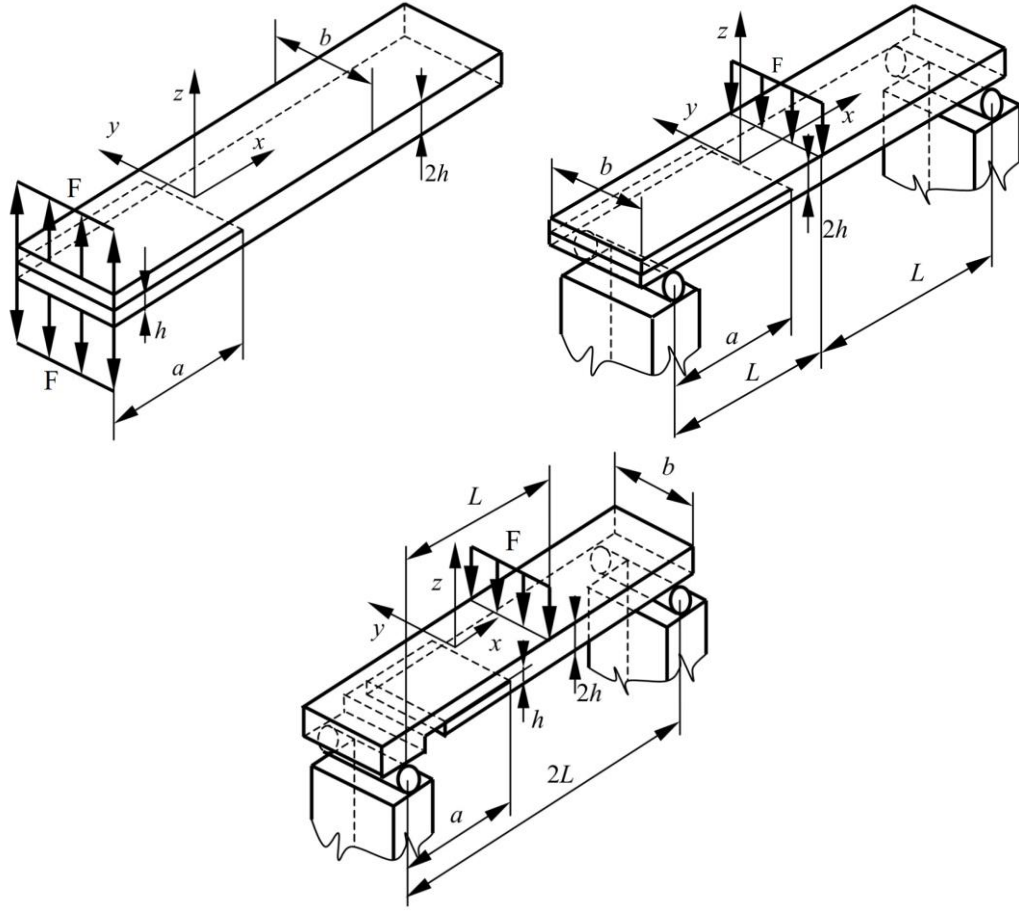
Figure 2: Standardised tests DCB (top left), ENF (top right) and MMF (bottom) [4]

Critical value of SERR for DCB test can be obtained using Euler-Bernoulli beam theory as

$$G_I^c = \frac{12F^2a^2}{bh^3E_x} = \frac{3F\delta}{2ba},\tag{4}$$

where $E_x$ is an effective Young's modulus in the direction of X-axis. For ENF test is the critical value mathematically described as

$$G_{II}^c = \frac{9F^2a^2}{16b^2h^3E_x} = \frac{3Fa^2\delta}{2b(3a^3 + 2L^3)}.\tag{5}$$

Analogically for test MMF

$$G_{I/II}^c = \frac{21F^2a^2}{16b^2h^3E_x} = \frac{672Fa^2\delta}{b(448a^3 + 121L^3)}.\tag{5}$$

**Finite element models**

Finite element model of standardized tests created in Abaqus CAE consist of two distinct parts: joined components and cohesive interface. Joined components are considered as linear elastic orthotropic material with following constitutive equation written for Cartesian material coordinate system as

$$
\begin{bmatrix} \sigma_1 \\ \sigma_2 \\ \sigma_3 \\ \sigma_4 \\ \sigma_5 \\ \sigma_6 \end{bmatrix} =
\begin{bmatrix}
\dfrac{E_1(1-\nu_{23}\nu_{32})}{\det(\boldsymbol{\nu})} & \dfrac{E_1(\nu_{21}+\nu_{23}\nu_{31})}{\det(\boldsymbol{\nu})} & \dfrac{E_1(\nu_{31}+\nu_{32}\nu_{21})}{\det(\boldsymbol{\nu})} & 0 & 0 & 0 \\
\dfrac{E_1(\nu_{21}+\nu_{23}\nu_{31})}{\det(\boldsymbol{\nu})} & \dfrac{E_2(1-\nu_{13}\nu_{31})}{det(\boldsymbol{\nu})} & \dfrac{E_2(\nu_{32}+\nu_{31}\nu_{12})}{\det(\boldsymbol{\nu})} & 0 & 0 & 0 \\
\dfrac{E_1(\nu_{31}+\nu_{32}\nu_{21})}{\det(\boldsymbol{\nu})} & \dfrac{E_2(\nu_{32}+\nu_{31}\nu_{12})}{\det(\boldsymbol{\nu})} & \dfrac{E_3(1-\nu_{12}\nu_{21})}{\det(\boldsymbol{\nu})} & 0 & 0 & 0 \\
0 & 0 & 0 & G_{23} & 0 & 0 \\
0 & 0 & 0 & 0 & G_{13} & 0 \\
0 & 0 & 0 & 0 & 0 & G_{12}
\end{bmatrix}
\begin{bmatrix} \varepsilon_1 \\ \varepsilon_2 \\ \varepsilon_3 \\ \varepsilon_4 \\ \varepsilon_5 \\ \varepsilon_6 \end{bmatrix}, \tag{6}
$$

where $\sigma_i$ is normal or shear stress, $\varepsilon_i$ is normal or shear strain, $E_i$ is Young's modulus, $G_{ij}$ is shear modulus and $\nu_{ij}$ is Poisson ratio [1]. Matrix $\boldsymbol{\nu}$ can be written as

$$
\boldsymbol{\nu} = \begin{bmatrix} 1 & -\nu_{12} & -\nu_{13} \\ -\nu_{12} & 1 & -\nu_{23} \\ -\nu_{13} & -\nu_{23} & 1 \end{bmatrix}. \tag{7}
$$

Cohesive interface is created by cohesive contact that is defined by a *bilinear traction-separation law* (visualized on figure 3), *quadratic stress criterion* (Eq. 8) and a *power law criterion* (Eq. 9) in each node of a contact pair.

$$
\left(\frac{t_{nn}}{t_{nn}^0}\right)^2 + \left(\frac{t_{ss}}{t_{ss}^0}\right)^2 + \left(\frac{t_{tt}}{t_{tt}^0}\right)^2 = 1, \tag{8}
$$

$$
\left(\frac{G_{nn}}{G_{nn}^c}\right)^\alpha + \left(\frac{G_{ss}}{G_{ss}^c}\right)^\alpha + \left(\frac{G_{tt}}{G_{tt}^c}\right)^\alpha = 1. \tag{9}
$$

*Traction-separation law* prescribes relation between stress component (normal/shear) and corresponding component of displacement. Surface under traction-separation curve is equal to critical value of SERR. *Quadratic stress criterion* defines failure of cohesive interface and *power law criterion* determines its damage initiation [3]. When power law criterion is fulfilled stiffness of interface is decreased (plastic strain is not present). For better understanding is this phenomenon described on figure 4.
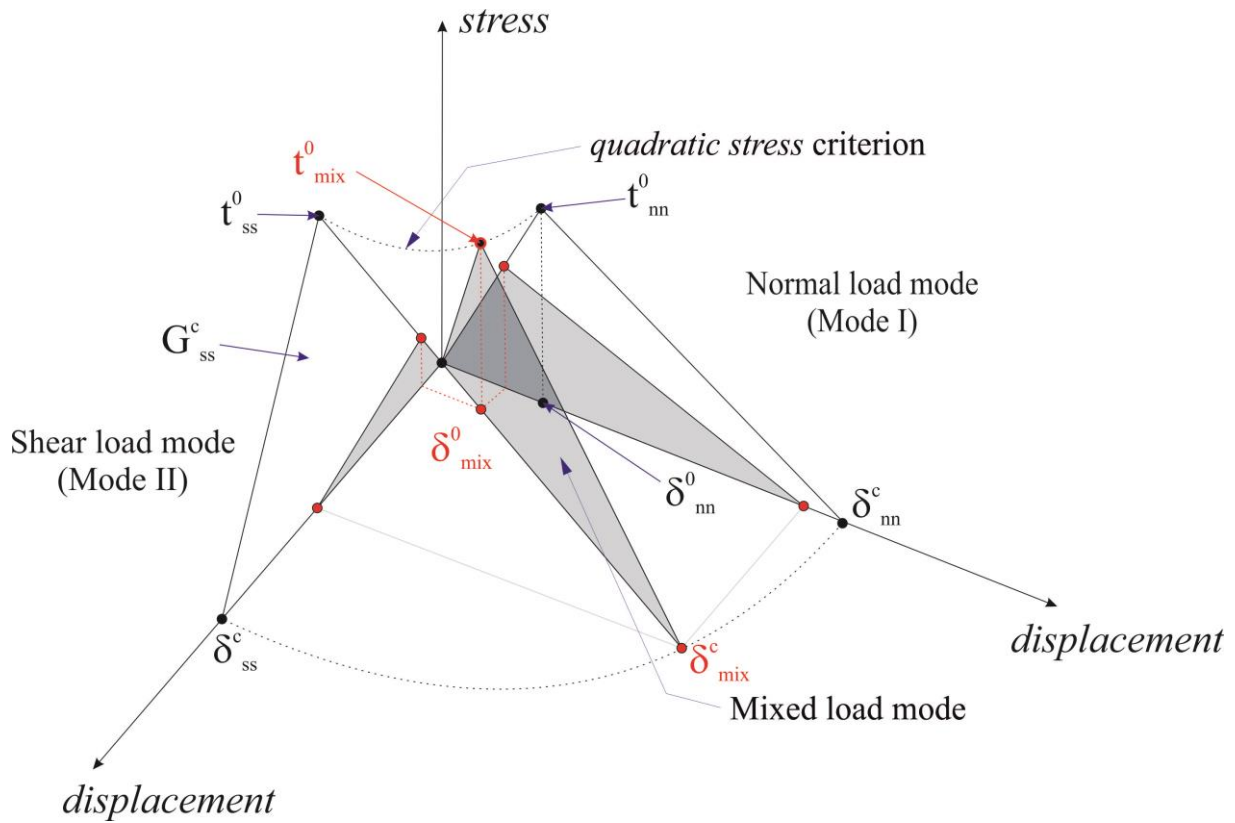
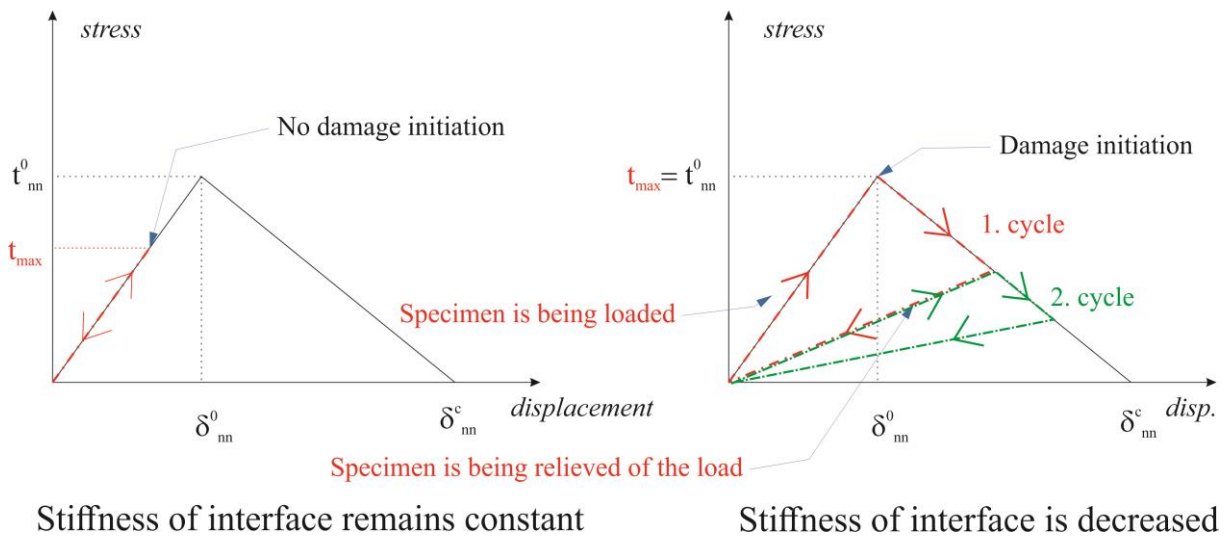Figure 3: Bilinear traction-separation law for combination of mode I and II



Figure 4: Power law criterion – visualization of damage initiation

**Realization**

Material parameters of cohesive interface were determined by standardized tests of an unidirectional carbon fibre-reinforced epoxy beams: DCB, ENF and MMF (mixed mode flexure). These three types of standardized test were performed to obtain dependence of force $F$ and displacement $\delta$ from loading point. As mentioned before failure analysis is based on identification of critical value of SERR $G^c$. Critical value of SERR extracted from experimental data is determined via analytical equations set for standardised tests stated above in section analytical model. Determination of load force $F$ is depicted on figure 5.
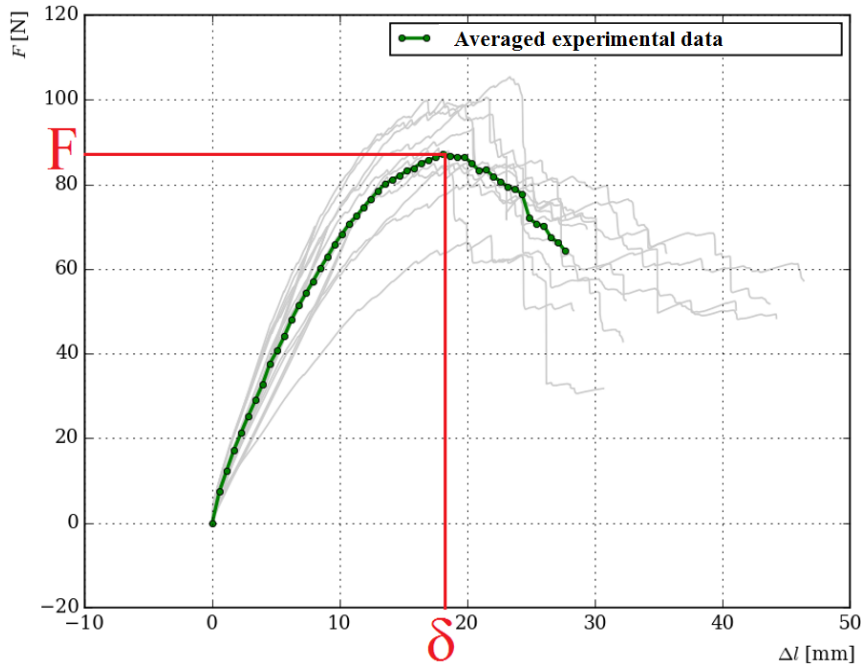


Figure 5: Determination of load force

Critical value of SERR obtained from FEA is determined through secondary material parameters of cohesive interface: stiffness $k$, displacement $\delta^0$ (damage initiation) and $\delta^c$ (failure determination). Secondary material parameters of cohesive interface were identified by comparison of force-displacement curves obtained from standardized tests and FE analysis. Comparison of force-displacement experimental and fitted FEA curves and visualisation of contact status change during load for corresponding model for DCB and ENF specimen with cohesive interface made of adhesive Araldite Hunstman 2021 is displayed on figure 6.
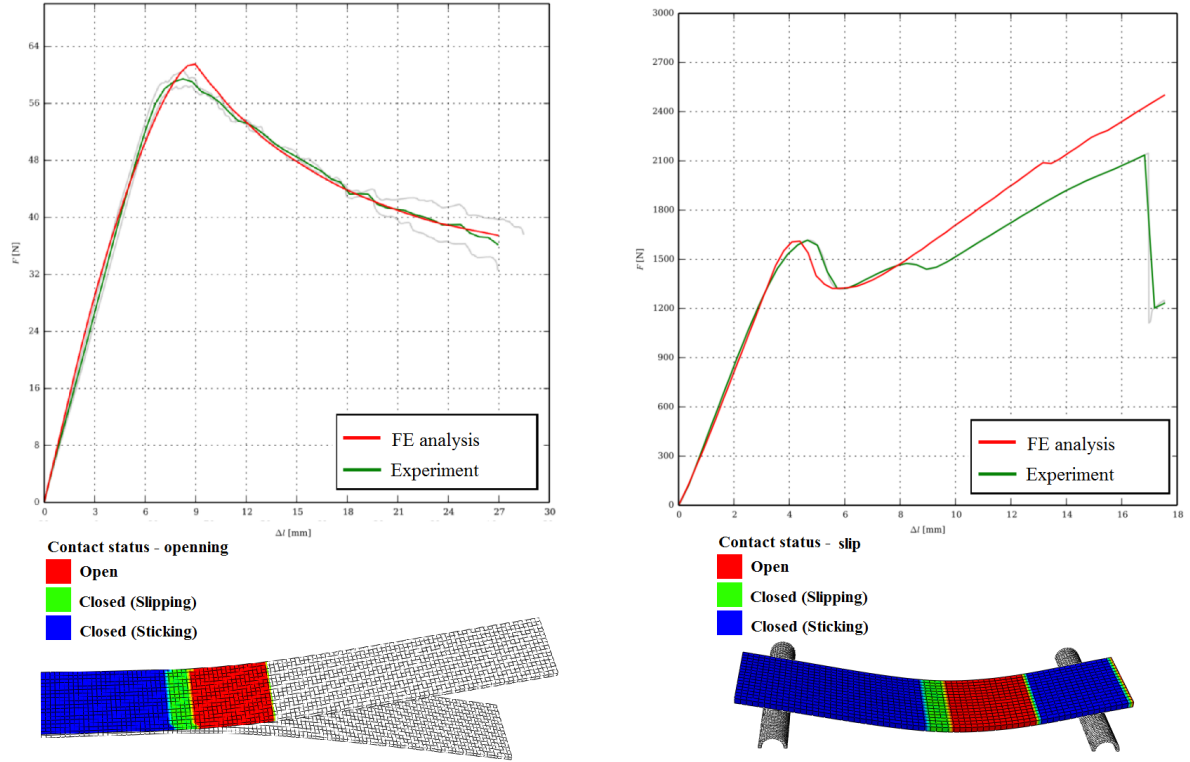
Figure 6: Comparison of force-displacement curves for DCB (left) and ENF specimen

This system of determination was chosen for its relative simplicity, because every parameter influences force-displacement curve in its own way. For e. g. effect of rising stiffness $k_{normal}$ on critical value of SERR and its effect on force-displacement curve (while remaining material parameters are constant) is depicted on figure 7 and effect of the $\delta^0_{shear}$ growth is depicted on figure 8.
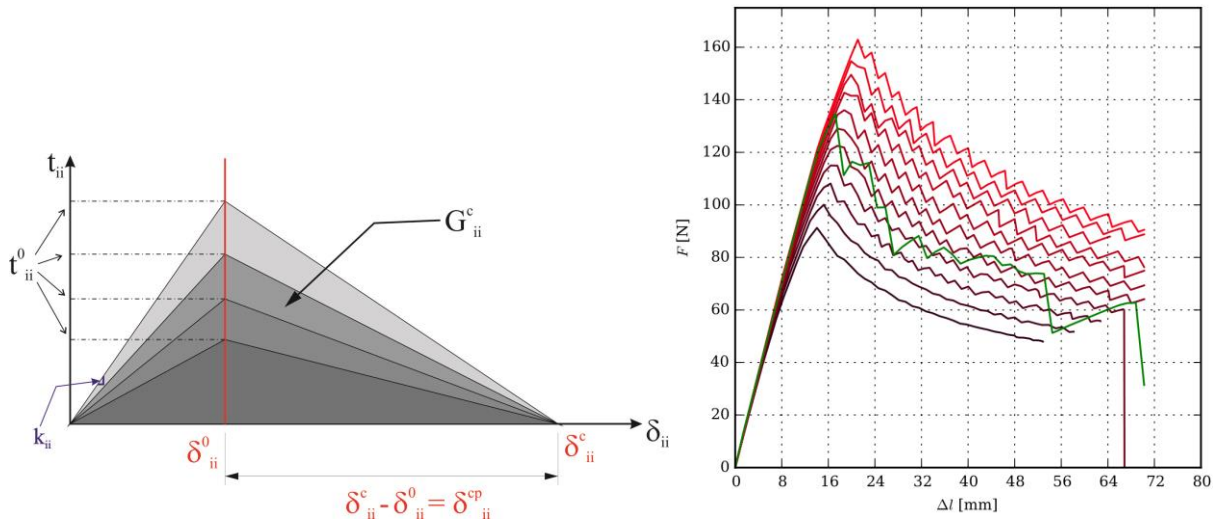


Figure 7: Influence of rising stiffness $k_{normal}$ on determination of $G^c$ for DCB test
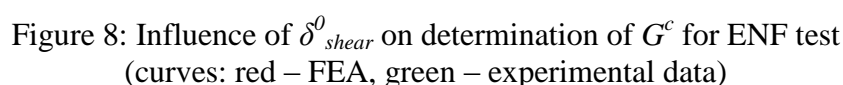(curves: red – FEA, green – experimental data)

Figure 8: Influence of $\delta^0_{shear}$ on determination of $G^c$ for ENF test
(curves: red – FEA, green – experimental data)

As mentioned before, material parameters of two adhesives (Hunstman Araldite 2021, Gurit Spabond 345) and inner layer of laminated composite were identified. Resultants for secondary material parameters can be found in table 1. Comparison of experimental and FEA critical value of SERR $G^c$ resultants is recorded in table 2.

Table 1: Resultants for secondary material parameters

| Mat. parameter | | Araldite | Spabond | Laminate |
|---|---|---|---|---|
| $k_{normal}$ | [GPa/m] | 32.0 | 42.0 | 24.0 |
| $k_{shear}$ | [GPa/m] | 72.0 | 100.0 | 100.0 |
| $\delta^0_{normal}$ | [μm] | 85.0 | 48.0 | 59.0 |
| $\delta^0_{shear}$ | [μm] | 155.0 | 220.0 | 30.0 |
| $\delta^c_{normal}$ | [μm] | 835.0 | 295.0 | 769.0 |
| $\delta^c_{shear}$ | [μm] | 395.0 | 350.0 | 450.0 |

Table 2: Comparison of experimental and FEA critical SERR resultants

| Experimental / FEA resultants of $G^c$ [J/m²] | DCB ($G_I{}^c$) | ENF ($G_{II}{}^c$) | MMF ($G_{I/II}{}^c$) |
|---|---|---|---|
| **Adhesive Gurit Spabond 345** | 385/301 | 3750/3850 | --- |
| **Adhesive Hunstman Araldite 2021** | 1353/1135 | 2045/2204 | --- |
| **Inner layer of composite** | 535/544 | --- | 730/--- |

**Conclusion**

Standardised tests DCB and ENF seems to be reliable tools for identification of failure defining material parameters for previously mentioned cohesive interfaces. MMF test alone is insufficient for determination of material parameters describing load mode II. Critical values of SERR, obtained from analytical equations and FEA, show agreement.

**Acknowledgement**

**References**

[1]    Laš, V., 2008. *Mechanika kompozitních materiálů.* University of West Bohemia, Faculty of Applied Sciences, Pilsen, Czech Republic.

[2]    Li C.F., Hu N., Yin Y.J., Sekine H.,Fukunaga H., 2002. *Low-velocity impact-induced damage of continuous fiber-reinforced composite laminates. Part 1. An FEM numerical model.*, Composites Part A str. 1055 - 1062

[3]    Reeder, J. R., 2006. *3D Mixed-Mode Delamination Fracture Criteria – An Experimentalist's Perspective.* NASA Langley Research Center, Hampton.

[4]    Szekrényes A., 2005. *Delamination of composite speciments*, Ph. D. dissertation, Budapest University of Technology and Economics, Budapest, Hungary.